Military Technical College
Kobry El-Kobbah,
Cairo, Egypt

I.C.E.E.2018

9th International Conference on Chemical & Environmental Engineering
3-5 April 2018

NCA-4

Mn_2O_3/Ag Nanoflakes as an Effective Electroscatalyst for Urea Oxidation in Alkaline Medium

Gehan M. K. Tolba

Abstract

In this study, highly crystalline Ag-doped Mn_2O_3 nanoflakes were synthesized by a sol-gel process and used as an effective electrocatalyst for urea electrooxidation in alkaline-media fuel cells. Scanning electron microscope (SEM), X-ray diffraction (XRD), transmission electron microscope (TEM) and energy dispersive spectroscopy (EDS) were applied to characterize the structure and the morphology of the final product. The electrocatalytic performances were investigated by cyclic voltammetry (CV) and chronoamperometry (CA) tests.The prepared nanocatalyst shows a distinct electrocatalytic activity toward urea oxidation. The introduced Ag-doped Mn_2O_3 reveals a good stability at various applied voltages. The enhanced electrocatalytic oxidation of urea using Ag-doped Mn_2O_3 nanoflakes reveals a great potential for future applications in hydrogen production, remediation of urea-rich wastewater, and fuel cells.

Keywords:
Nanosilver; Nanoparticles; Urea; Electooxidation; Electrocatalyst; Fuel cells

Chemical Engineering Department, Faculty of Engineering, Minia University, Minia, Egypt

Military Technical College
Kobry El-Kobbah,
Cairo, Egypt

I.C.E.E.2018

9th International Conference on Chemical & Environmental Engineering
3-5 April 2018

1. Introduction

The consumption of energy in the 20th century has increased exponentially. According to the US Energy Information Administration, the global energy consumption in 2006 was approximately 500 EJ. In addition, the consumption is expected to increase to 720 EJ by 2030. The energy from fossil fuels such as coal, oil, and natural gas was estimated by about 86% from the total energy. These sources are not renewable and emit greenhouse gases that contribute to the global warming [1, 2]. Development of advanced energy technology might be participating in solving this problem. The most promising alternatives to fossil fuels are hydrogen storage, fuel cells, DSSCs, lithium ion batteries, and supercapacitors [3-6]. These new types of energy are more efficient, cost effective, and clean. However, these types still need a performance enhancement for increasing conversion efficiency, harvest efficiency, and power density [7, 8].

Urea is a non-toxic, stable, and widely available inexpensive industrial product, which is widely used as an animal feed additive and nitrogen-release fertilizer in the agricultural industry. Large volumes of wastewater with different urea concentration are formed during the industrial synthesis of urea and human/animal urine. The untreated urea-rich wastewater has a harmful effect on the environment, which can go through a natural conversion to toxic ammonia and then emitted to the atmosphere. It also poses dangers to the ground and drinking water that causes health problems [2, 9]. Suitable methods for urea removal or decomposition during treatment of wastewater are therefore necessary for both environmental and energy issues. Production of hydrogen from urea-rich wastewater by electrolysis has been recently reported as a promising and more efficient approach for urea removal owing to its great potential application in fuel cells, hydrogen production, and wastewater remediation. The energy density of urea (16.9 MJ/L) is higher than compressed or liquid hydrogen, which makes it a potential energy carrier. If an adult human produces 1.5 L of urine containing 2 wt% urea, it would produce 11 kg of urea each year, which is equivalent to the energy in 18 kg of liquid hydrogen that can be used to drive a car for 2700 km if powered by a urea fuel cell [9-11].

A fuel cells are electrochemical devices which convert directly chemical energy to electricity by oxidizing a fuel at the anode and reducing air (O_2) catalyzed by immobilized electrode material with high efficiency. Low-temperature fuel cell has particularly been attracting attention because of its important applications in electronic devices like cellular phones, cameras, laptops, and camcorders. Direct urea fuel cells would be an effective technique for generating electricity from wastewater containing fertilizer urea or urine using urea or urine as the fuel. Which urea was electrochemically

Military Technical College
Kobry El-Kobbah,
Cairo, Egypt

I.C.E.E.2018

9th International Conference on Chemical & Environmental Engineering
3-5 April 2018

oxidized to nitrogen gas and converted into carbonate at the anode, removing it from urine [12, 13].

A key requirement for urea electrooxidation is to investigate highly efficient and economic electrocatalysts. Research has shown that urea can be electrochemically oxidized in a neutral medium using noble-metal catalyst such as platinum because of its unique catalytic property. However, the high cost of platinum and severe surface poisoning during electrocatalysis have limited its practical applications. Therefore, great advances have been achieved to minimize usage of high cost noble metals and prevent surface poisoning by developing various materials including inexpensive transition metal-based catalysts. Several studies indicated that nanostructured nickel catalysts or nickel-based multi-metal catalysts can enhance the urea oxidation reaction for hydrogen production because of its large surface areas, or its synergistic effect of the multi-element catalysts. Moreover, they introduced higher current densities and lower oxidation potentials for the oxidation of urea than those of the noble-metal catalysts [14].

There is a potential gap between the theoretical and the detected electro-oxidation potential of urea when using pure Ni catalysts. The presence of a large overpotential, and therefore high potential, for the electrooxidation of urea decreases the efficiency of the urea electrolysis process, and causes a certain degree of the oxygen evolution reaction (OER) in alkaline fuel cell media [15, 16]. The OER in alkaline media will not only leads to further energy loss for urea electrolysis, but also makes a negative impact on the stability of the nickel electrode. Therefore, novel catalysts are need to be investigated to promot urea electrooxidation, reduce the urea oxidation potential, and decrease the interference of the OER. Designing an effective electrocatalyst for the urea oxidation to be used as anode is not an easy task.

One such important functional metal oxide is Mn_2O_3, which has captured the interest of many researchers owing to its wide applications [17-19]. Its higher surface area is especially of great significance for catalytic applications. Beside silver is known to be a powerful, natural antimicrobial agent preventing serious infections. Ag nanoparticles (AgNP) have been shown to exhibit interesting catalytic, antibacterial and biosensing properties. The doping of metal ions into the manganese oxide lattice can be useful, as manganese oxide can be easily prepared, it is environmental-friendly, easy to handle and very economical. Also, these doped manganese oxides materials were found to shows a good catalytic activity [17, 20, 21].

Military Technical College
Kobry El-Kobbah,
Cairo, Egypt

I.C.E.E.2018

9th International Conference on Chemical & Environmental Engineering
3-5 April 2018

In this study, Ag-doped Mn_2O_3 nanoflakes were synthesized and the effectiveness of the produced catalyst toward urea electrooxidation in a direct urea fuel cell was investigated. The performances of the Ag-doped Mn_2O_3 nanoflakes catalyst for the urea electrooxidation were investigated and evaluated by cyclic voltammetry (CV). The resulting catalyst shows an excellent catalytic activity and an outstanding stability for urea oxidation in an alkaline medium.

2. Experimental

2.1 Materials

Silver nitrate ($AgNO_3$; 99.0 % assay) was obtained from Sigma Aldrich and manganese acetate tetrahydrate (MnAc; 98% assay) was obtained from Alfa Aesar. Both were utilized as precursors. Citric acid was purchased from SamChun Chem. Co., South Korea and utilized as a gelling agent for gel production. All chemicals were used as received without further purification.

2.2 Catalyst synthesis

Ag/Mn_2O_3 nanoflakes were prepared as follows. In brief, 12 g of MnAc and 0.2 g of $AgNO_3$ were dissolved into 100 mL deionized water under constant stirring. Then, 9 g citric acid was added as a gelling agent into the above solution with continuous stirring. The pH was maintained at 7 by adding ammonia solution drop-wisely. The mixture was allowed to stirring for 4 h. After the formation of a homogeneous gel, the mixture was dried at 80 $^{\circ}$C and then grinded. The obtained powder was calcined at 600 $^{\circ}$C for 2 h.

2.3 Characterization

The surface morphology was studied by a JEOL JSM-5900 scanning electron microscope (JEOLLtd., Japan) and field-emission scanning electron microscope (FE-SEM, Hitachi S-7400, Japan). Moreover, the phase and crystallinity of the catalyst were characterized using a Rigaku X-ray diffractometer (Rigaku Co., Japan) with Cu Kα (λ=1.54056 Å) radiation over a range of 2θ angles from 20^o to 80^o. In addition, normal and high resolution images were obtained with transmission electron microscope (TEM, JEOL JEM-2010, Japan) operated at 200 kV equipped with EDX analysis. Cyclic voltammetry measurements were conducted by VersaStat4 potentiostat device. The electrochemical measurements were carried out in alkaline medium solution (1.0 M KOH) by using a conventional three-electrode electrochemical cell. A Pt wire, an Ag/AgCl and glassy carbon electrodes were used as the auxiliary, reference and working electrodes, respectively. All potentials were quoted regarding to the Ag/AgCl electrode. Moreover, preparation of the working electrode was carried out by mixing 2 mg of the functional

material, 20 µL Nafion solution (5 wt%) and 400 µL isopropanol. Additionally, the slurry was sonicated for 10 min at room temperature. A volume of 15 µL from the prepared slurry was poured on the active area of the glassy carbon electrode which was dried at 80 ^{o}C for 20 min.

3. Results and discussion

3.1 Characterization of Ag-doped Mn_2O_3 nanoflakes

Figure 1A and 1B display SEM and FE-SEM images of the obtained Ag-doped Mn_2O_3 powder, respectively. As shown in the figures, the attained product in the form of nanoflakes. Although the size of the obtained powder is not uniform, most of it is of nanosize all is in the nanosize. However, some agglomeration can be detected in the FE-SEM image (Fig.2B). It is well-known that during the sintering of ceramic materials they tend to agglomerate [22]. Specifically, refractory high tendency metal oxides by forming sintered products, however the image shows quite numerous very thin flakes in the nanoscale, which makes the naming of the obtained product as nanoflakes reliable.

The typical X-ray diffraction (XRD) patterns of the obtained Ag-doped Mn_2O_3 are presented in Figure 2. As shown in the figure, the diffraction peaks at 2θ values of 38.1°, 44.2°, 64.2°, and 77.5° assigned to (111), (200), (220), and (311) crystal planes, respectively indicate the formation of cubic structure Ag (Sp.Gr Fm (225), JCPDS 04-0783). Moreover, the standard peaks of Mn_2O_3 are clearly appeared in the pattern. The diffraction peaks appeared at 2θ of 18.8°, 32.9°, 38.3°, 45.2°, 55.2° and 65.8° corresponding to (220), (222), (400), (332), (440) and (622), respectively affirm the formation of cubic Bixbyite-C Mn_2O_3 (Sp.Gr Fm (206), JCPDS 41-1442). Moreover, no other peaks referring to other compounds can be seen which indicates that the obtained product composes of Ag and Mn_2O_3.

Transition electron microscope (TEM) is applied to investigate the inner structure of the obtained product. Figure 3A shows the normal TEM image of the obtained product. As shown in the figure, there are numerous small dark spots (nanoparticles) dispersed in/on the nanoflake matrix. The high-resolution TEM image (Figure 3B) further demonstrates that the silver nanoparticles are loaded onto the manganese oxide matrix in highly crystalline structure. As shown in the figure, the lattice distance almost matches the standard lattice parameter of Mn_2O_3, which confirms that the main body of the introduced nanoflakes is manganese oxide. And the observed small nanoparticles distributed along with the metal oxide matrix have different lattice parameters marked by the red circles.

Military Technical College
Kobry El-Kobbah,
Cairo, Egypt

I.C.E.E.2018

9th International Conference on Chemical & Environmental Engineering
3-5 April 2018

Accordingly, these nanoparticles can be assigned as silver nanoparticles. Therefore, it is safe to claim that the produced product is Ag nanoparticles-doped Mn_2O_3 nanoflakes.

.

3.2 Electrochemical measurements

3.2.1 Urea oxidation

Figure 4 displays the cyclic voltammetric behavior of the prepared Ag-doped Mn_2O_3 in presence and absence of urea (0.5 M) in 1.0 M KOH solution. A scanning rate of 100 mV/s from 800 mV to 0 mV Polarization was started by a potential scanning at a scan rate of 50 mVs^{-1} from 1000 to -200 mV (vs. Ag/AgCl reference electrode). As shown in the figure, presence of urea increases the anodic current density at potential higher than 500 mV (vs. Ag/AgCl) which indicates the strong electrocatalytic activity of the introduced electrocatalyst for urea oxidation. Moreover, a considerable decrease in the cathodic current density can be observed during the reverse scan. The high increase in the anodic peak followed by the considerable decrease in the cathodic peak in the reverse scan is consistent with a behavior typical to the catalytic regeneration effect [23].

As the surface of the obtained nanoflakes is doped by Ag, it is expected that the introduced electrocatalyst does not need activation by forming an active layer on the surface such as Ni-based electrocatalysts. To affirm this hypothesis, cycling voltammetry in the presence of 1 M KOH has been performed for several cycles. Figure 5 indicates the CV data for the cleaning step of the electrocatalyst electrode in 1 M KOH at 25 ˚C. As shown, redox indicates that the obtained nanoflakes do not need any activation.

3.2.2 Influence of urea solution concentration

The influence of urea concentration on the catalytic performance of the Ag-doped Mn_2O_3 electrode was investigated. Figure 6 displays CV of Ag-doped Mn_2O_3 as anode at different urea concentration with scan rate of 50 mV/s and applied potentials between 1000 to -0.200 mV. As shown in the figure the current density increases with increasing the urea concentration up to 0.5 M. After that more increase in the urea concentration leads to a slight decrease in current density. At low urea concentration (up to 0.5 M), it could be hypothesized that the increase in the anodic current density is due to a diffusion-controlled process. However, after urea concentration of 0.5 M, there is almost no change in the anodic current density as the current density was independent on the urea concentration, which may be due to the kinetics-limitation control process. This finding indicates that the surface coverage of urea molecules becomes high at high concentrations; accordingly, a fixed oxidation rate is observed due to the local deprivation of OH^- for the extra urea molecules. Another important finding is that an increase in the urea concentration leads to a slight increase in the urea oxidation potential. Increasing the urea concentration leads to increasing the surface coverage of urea and/or

the intermediates, thus leading to a high current density by oxidizing large amount of adsorbed molecules. In addition, the adsorbed OH^- coverage on the catalyst surface will decrease due to the high coverage of the surface by urea and intermediates**.** Therefore, the optimum urea concentration is 0.5 M as could be concluded from the figure.

3.2.3 Catalyst stability

Chronoamperometric experiments were performed to evaluate the stability of the catalysts. The experiments took place at a constant voltage of 0.7 V, which is the peak potential of urea oxidation on the Ag-doped Mn_2O_3 electrode for 11 h **(Figure 7)** . As shown in the figure that the electrocatalyst shows a continuous behavior , and almost constant trend during the whole testing period, which indicates that Ag-doped Mn_2O_3 is active and stable for urea electrooxidation in alkaline medium.

4. Conclusion

Highly crystalline Ag-doped Mn_2O_3 nanoflakes were produced via a sol-gel process using silver nitrate and manganese acetate as precursors, and citric acid as a gelatinizing agent. However, the obtained sol-gel should be carefully dried, grinded and calcined in air. The introduced Ag-doped Mn_2O_3 nanoflakes can be exploited as an effective catalyst toward urea electrooxidation. Consequently, indicating promising applications in remediation of urea-rich wastewater and fuel cells.

5. References

[1] M. Bazilian, P. Nussbaumer, H.-H. Rogner, A. Brew-Hammond, V. Foster, S. Pachauri, E. Williams, M. Howells, P. Niyongabo, L. Musaba, Energy access scenarios to 2030 for the power sector in sub-Saharan Africa, Utilities Policy, 20 (2012) 1-16.

[2] Z. Dong, S.J. Kennedy, Y. Wu, Electrospinning materials for energy-related applications and devices, Journal of Power Sources, 196 (2011) 4886-4904.

[3] Y.G. Guo, J.S. Hu, L.J. Wan, Nanostructured materials for electrochemical energy conversion and storage devices, Advanced Materials, 20 (2008) 2878-2887.

[4] M. Winter, R.J. Brodd, What are batteries, fuel cells, and supercapacitors?, in, ACS Publications, 2004.

[5] P. Thounthong, S. Rael, B. Davat, Energy management of fuel cell/battery/supercapacitor hybrid power source for vehicle applications, Journal of Power Sources, 193 (2009) 376-385.

Military Technical College
Kobry El-Kobbah,
Cairo, Egypt

I.C.E.E.2018

9th International Conference on Chemical & Environmental Engineering
3-5 April 2018

[6] P. Thounthong, S. Raël, B. Davat, Control strategy of fuel cell and supercapacitors association for a distributed generation system, IEEE Transactions on Industrial Electronics, 54 (2007) 3225-3233.
[7] H. Wang, H. Dai, Strongly coupled inorganic–nano-carbon hybrid materials for energy storage, Chemical Society Reviews, 42 (2013) 3088-3113.
[8] D. Wang, W. Yan, S.H. Vijapur, G.G. Botte, Electrochemically reduced graphene oxide–nickel nanocomposites for urea electrolysis, Electrochimica Acta, 89 (2013) 732-736.
[9] E. Urbańczyk, M. Sowa, W. Simka, Urea removal from aqueous solutions—a review, Journal of Applied Electrochemistry, 46 (2016) 1011-1029.
[10] D. Wang, W. Yan, S.H. Vijapur, G.G. Botte, Enhanced electrocatalytic oxidation of urea based on nickel hydroxide nanoribbons, Journal of power sources, 217 (2012) 498-502.
[11] E.H. Yu, X. Wang, U. Krewer, L. Li, K. Scott, Direct oxidation alkaline fuel cells: from materials to systems, Energy & Environmental Science, 5 (2012) 5668-5680.
[12] R. Lan, S. Tao, Preparation of nano-sized nickel as anode catalyst for direct urea and urine fuel cells, Journal of Power Sources, 196 (2011) 5021-5026.
[13] W. Xu, H. Zhang, G. Li, Z. Wu, Nickel-cobalt bimetallic anode catalysts for direct urea fuel cell, Scientific reports, 4 (2014) 5863.
[14] R. Ding, L. Qi, M. Jia, H. Wang, Facile synthesis of mesoporous spinel $NiCo_2O_4$ nanostructures as highly efficient electrocatalysts for urea electro-oxidation, Nanoscale, 6 (2014) 1369-1376.
[15] L. Wang, M. Li, Z. Huang, Y. Li, S. Qi, C. Yi, B. Yang, Ni–WC/C nanocluster catalysts for urea electrooxidation, Journal of Power Sources, 264 (2014) 282-289.
[16] L. Wang, T. Du, J. Cheng, X. Xie, B. Yang, M. Li, Enhanced activity of urea electrooxidation on nickel catalysts supported on tungsten carbides/carbon nanotubes, Journal of Power Sources, 280 (2015) 550-554.
[17] R. Kunkalekar, A. Salker, Low temperature carbon monoxide oxidation over nanosized silver doped manganese dioxide catalysts, Catalysis Communications, 12 (2010) 193-196.
[18] S. Gnanam, V. Rajendran, Synthesis of CeO_2 or α–Mn_2O_3 nanoparticles via sol–gel process and their optical properties, Journal of sol-gel science and technology, 58 (2011) 62-69.
[19] G. Mohseni, M. Negahdary, H. Faramarzi, S. Mehrtashfar, A. Habibi-Tamijani, S.H. Nazemi, Z. Morshedtalab, M. Mazdapour, S. Parsania, Voltammetry behavior of modified carbon paste electrode with cytochrome C and Mn_2O_3 nanoparticles for hydrogen peroxide sensing, Int. J. Electrochem. Sci, 7 (2012) 12098-12109.

[20] R. Kunkalekar, M. Prabhu, M. Naik, A. Salker, Silver-doped manganese dioxide and trioxide nanoparticles inhibit both Gram positive and Gram negative pathogenic bacteria, Colloids and Surfaces B: Biointerfaces, 113 (2014) 429-434.
[21] Y. Wang, Y. Wang, D. Jia, Z. Peng, Y. Xia, G. Zheng, All-nanowire based Li-ion full cells using homologous Mn_2O_3 and $LiMn_2O_4$, Nano letters, 14 (2014) 1080-1084.
[22] A. Varma, A.S. Mukasyan, A.S. Rogachev, K.V. Manukyan, Solution combustion synthesis of nanoscale materials, Chemical reviews, 116 (2016) 14493-14586.
[23] K. Lida, R. Mohammad, S. Maryam, S. Hamidreza, Kinetic Study of the Oxidation of Catechols in the Presence of N-Methylaniline, Journal of Chemistry, 2013 (2012).

Military Technical College
Kobry El-Kobbah,
Cairo, Egypt

I.C.E.E.2018

9th International Conference on Chemical & Environmental Engineering
3-5 April 2018

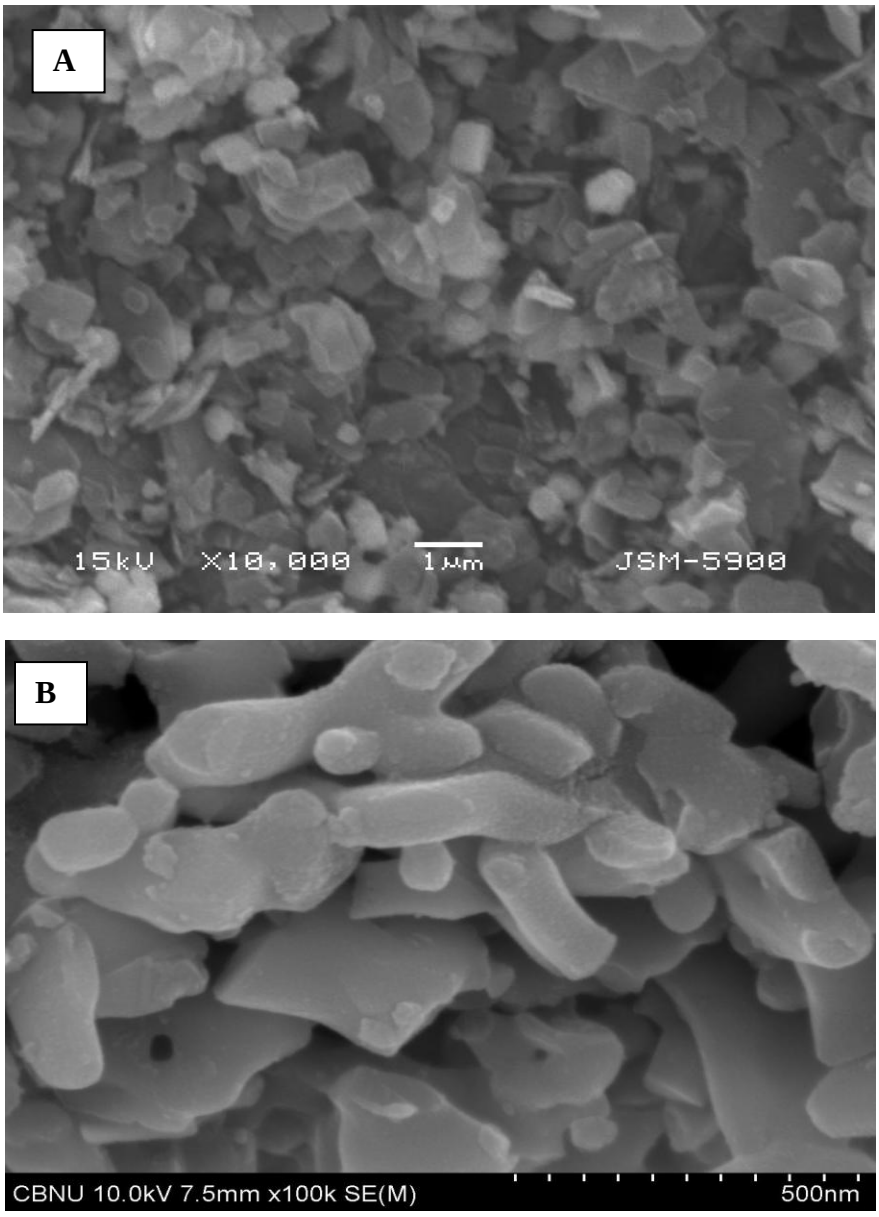

Figure 1 (A); SEM image (B); FE-SEM image of the obtained Ag-doped Mn_2O_3 nanoflakes

Military Technical College
Kobry El-Kobbah,
Cairo, Egypt

I.C.E.E.2018

9th International Conference on Chemical & Environmental Engineering
3-5 April 2018

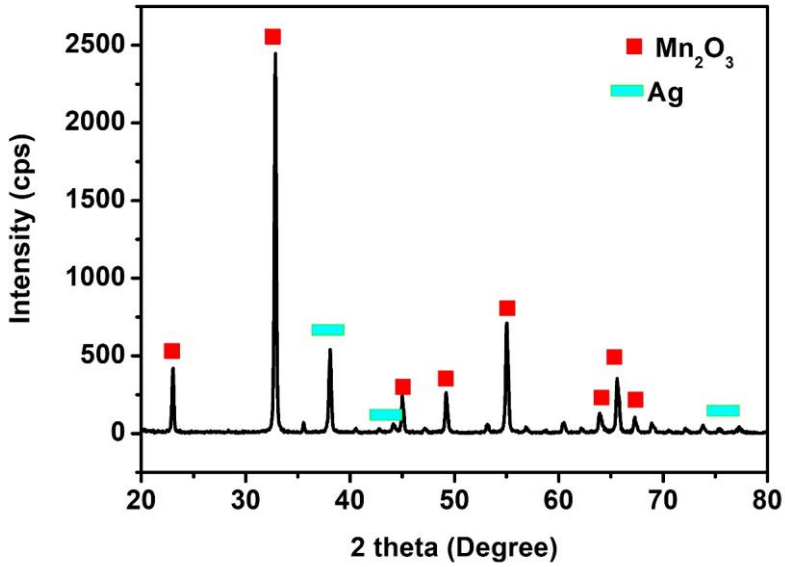

Figure 2 XRD pattern of the obtained Ag-doped Mn_2O_3 nanoflakes

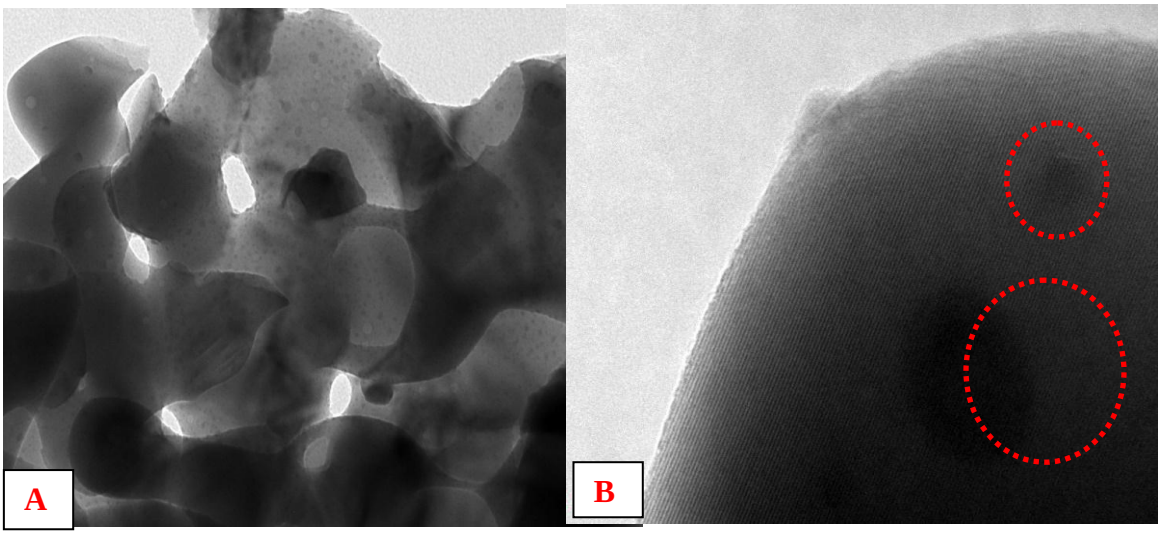

Figure 3 (A) Normal TEM image; and (B) HR TEM image; for the prepared Ag-doped Mn_2O_3 nanoflakes

Military Technical College
Kobry El-Kobbah,
Cairo, Egypt

I.C.E.E.2018

9th International Conference on Chemical & Environmental Engineering
3-5 April 2018

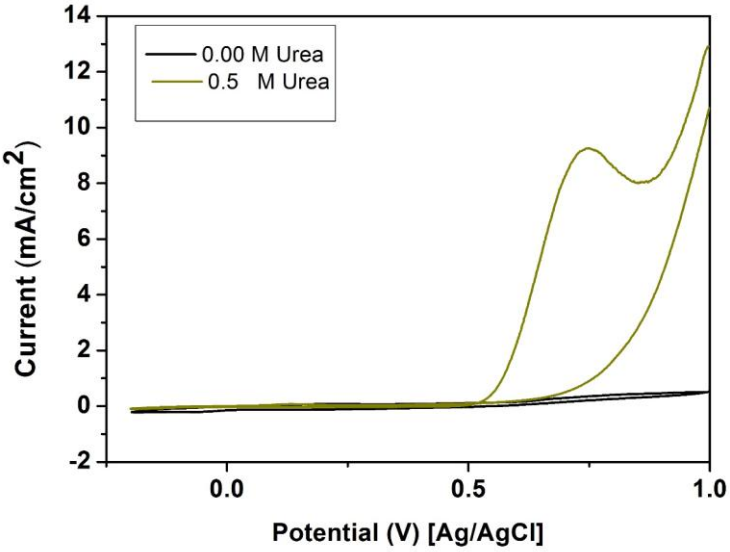

Figure 4 Cyclovotammogram for the obtained Ag-doped Mn_2O_3 nanoflakes in the presence and absence of urea: 1.0 M KOH, 50 mV/s scan rate and 25 ˚C.

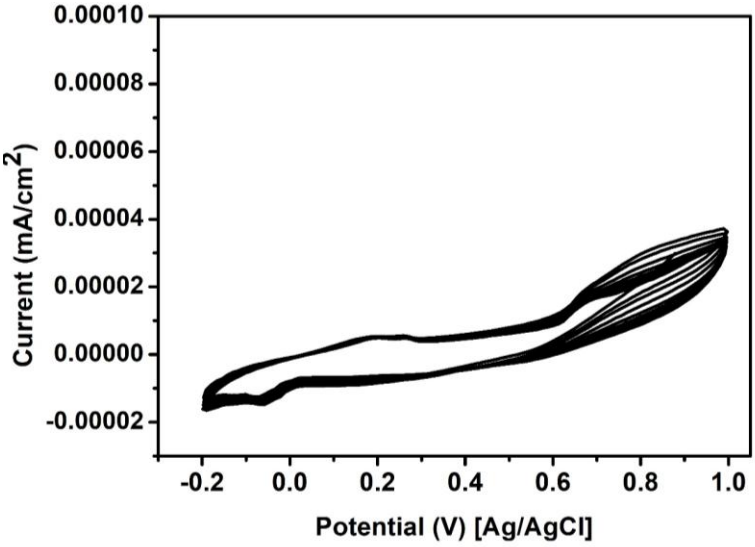

Figure 5 Cyclic voltammograms at a scan rate of 50 mV/s and 25 ˚C for the obtained Ag-doped Mn_2O_3 nanoflakes in 1 M KOH.

Military Technical College
Kobry El-Kobbah,
Cairo, Egypt

I.C.E.E.2018

9th International Conference on Chemical & Environmental Engineering
3-5 April 2018

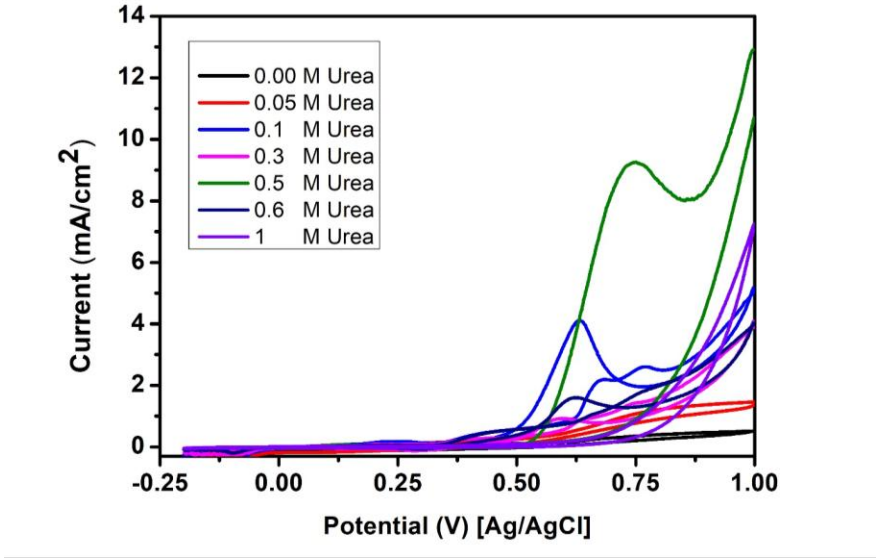

Figure 6 Cyclic voltammograms at a scan rate of 50 mV/s and 25˚C for the obtained Ag-doped Mn_2O_3 nanoflakes with different urea concentrations (in 1 M KOH).

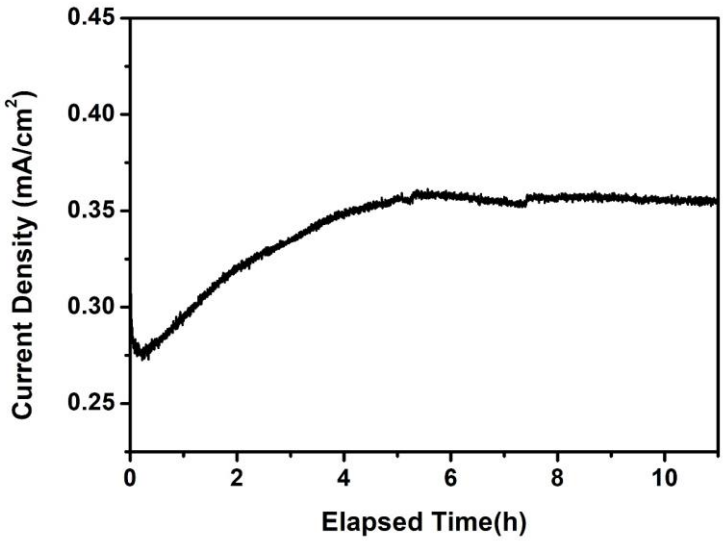

Figure 7 Constant voltage tests of the obtained Ag-doped Mn_2O_3 nanoflakes at a cell potential of 0.7 V and 0.5 M urea. The cell temperature was 25 ˚C.